

This article was published in an Elsevier journal. The attached copy is furnished to the author for non-commercial research and education use, including for instruction at the author's institution, sharing with colleagues and providing to institution administration.

Other uses, including reproduction and distribution, or selling or licensing copies, or posting to personal, institutional or third party websites are prohibited.

In most cases authors are permitted to post their version of the article (e.g. in Word or Tex form) to their personal website or institutional repository. Authors requiring further information regarding Elsevier's archiving and manuscript policies are encouraged to visit:

<http://www.elsevier.com/copyright>



# Searching for switchable molecular conductors: Salts of $[M(\text{dcbdt})_2]$ ( $M = \text{Ni}, \text{Au}$ ) anions with $[\text{Fe}(\text{sal}_2\text{-trien})]^+$ and $[\text{Fe}(\text{phen})_3]^{2+}$

L.C.J. Pereira, A.M. Gulamhussen, J.C. Dias, I.C. Santos, M. Almeida \*

*Departamento de Química, ITN/CFMCUL, E.N. 10, P-2686-953 Sacavém, Portugal*

Received 26 November 2006; received in revised form 7 March 2007; accepted 7 March 2007

Available online 19 March 2007

Paper presented in the MAGMANet-ECMM, European Conference on Molecular Magnetism.

## Abstract

Salts of  $[\text{Fe}^{\text{III}}(\text{sal}_2\text{-trien})]^+$  and  $[\text{Fe}^{\text{II}}(\text{phen})_3]^{2+}$  cations and  $[M(\text{dcbdt})_2]^-$  anions with  $M = \text{Ni}$  and  $\text{Au}$  ( $\text{dcbdt} = \text{dicyanobenzenedithiolate}$ ) with formula  $[\text{Fe}(\text{sal}_2\text{-trien})][M(\text{dcbdt})_2]$  and  $[\text{Fe}(\text{phen})_3][M(\text{dcbdt})_2]$  were obtained and characterized by single X-ray diffraction and magnetic measurements. None of these salts shows a clear spin crossover behaviour and their magnetic properties are due essentially to the cations in a high spin  $S = 5/2$  and low spin states for the  $\text{Fe}^{\text{III}}$  and  $\text{Fe}^{\text{II}}$  salts respectively. The magnetic Ni sublattices in both compounds appear to have a negligible direct contribution to the magnetization but enhance the AF interactions in the cation sublattice. © 2007 Elsevier B.V. All rights reserved.

**Keywords:** Fe complexes; Magnetic properties

## 1. Introduction

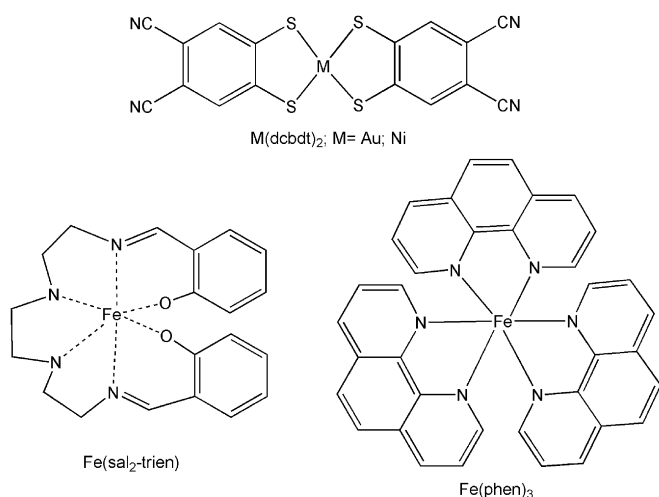
Recently there has been an increasing interest in achieving molecular conducting systems in which the electrical conducting properties can be modulated by variations in the spin state of spin cross-over units incorporated in such a solid. Using a hybrid molecular approach such type of materials could be achieved in a salt, by combination of a spin crossover system, with appropriated molecules which in the solid state may form electrically conducting partially oxidized extended networks.

Since the spin crossover compounds known so far are essentially cationic complexes, mainly of  $\text{Fe}^{\text{II}}$  or  $\text{Fe}^{\text{III}}$  [1], this hybrid approach implies that the conducting network is based on anionic species. Indeed in an attempt to achieve hybrid conducting materials some Fe spin crossover cations such as  $[\text{Fe}(\text{sal}_2\text{-trien})]^+$  ( $\text{sal}_2\text{-trien}$  is the ligand obtained from the condensation of two molecules of sali-

cylaldehyde and triethylamine) have been recently combined with anionic  $[M(\text{dmit})_2]^{n-}$  complexes ( $\text{dmit} = 1,3\text{-dithiole-2-thione-4,5-dithiolate}$ ) [2,3]. The  $[M(\text{dmit})_2]$  complexes are well known as capable of forming in the solid state partially oxidized extended networks which are at the base of several molecular metals and even superconductors [4]. However, the compounds obtained so far with  $[M(\text{dmit})_2]$  anions are at most semiconductors with modest electrical conductivity, and in some cases the spin transitions are absent.

In this context it is important to explore new compounds with spin crossover cations and other molecules capable of making anionic conducting networks. We have previously described another type of anionic transition metal bisdithiolene complexes,  $[M(\text{dcbdt})_2]$  ( $\text{dcbdt} = \text{dicyanobenzenedithiolate}$ ) which can exist in a variety of oxidation states [5], including partially oxidised ones associated with high electrical conductivity, such as in  $[n\text{-Bu}_4\text{N}][M(\text{dcbdt})_2]$   $M = \text{Ni}, \text{Au}$  [6]. In this paper we describe new charge transfer salts of  $[M(\text{dcbdt})_2]$  anions with  $M = \text{Au}$  and  $\text{Ni}$  with the  $\text{Fe}^{\text{III}}$  and  $\text{Fe}^{\text{II}}$  cations  $[\text{Fe}(\text{sal}_2\text{-trien})]^+$  and  $[\text{Fe}(\text{phen})_3]^{2+}$  (see Scheme 1).

\* Corresponding author. Tel.: +351 219946171; fax: +351 2199414155.  
E-mail address: [malmeida@itn.pt](mailto:malmeida@itn.pt) (M. Almeida).



Scheme 1.

## 2. Experimental

### 2.1. Synthesis

The salts (*n*-Bu<sub>4</sub>N) [Ni(dcbdt)<sub>2</sub>] and (*n*-Bu<sub>4</sub>N) [Au(dcbdt)<sub>2</sub>] were prepared by using the procedures previously reported [5]. The salts [Fe(sal<sub>2</sub>-trien)] (PF<sub>6</sub>) and [Fe(Phen)<sub>3</sub>] (PF<sub>6</sub>)<sub>2</sub> were prepared as described in the literature by Tweedle and Wilson [7] and Decurtins et al. [8]. All solvents were dried under nitrogen prior to use. Elemental analyses were performed by the analytical services of ITN.

DMF, acetonitrile, and dichloromethane were distilled from phosphorus pentoxide, while benzene was distilled from sodium prior to use. All other reagents were used without further purification.

#### 2.1.1. [Fe(sal<sub>2</sub>-trien)] [Au(dcbdt)<sub>2</sub>] (1)

A solution of [Fe(sal<sub>2</sub>-trien)] (PF<sub>6</sub>) (17.00 mg, 3.06 × 10<sup>−2</sup> mmol) in 20 mL of acetonitrile was added dropwise to a solution of (*n*-Bu<sub>4</sub>N) [Au(dcbdt)<sub>2</sub>] (20.40 mg, 2.49 × 10<sup>−2</sup> mmol), in the same amount of the same solvent. Slow evaporation under nitrogen flow gave 19.41 mg of black parallelepipedic crystals, which were washed with cold acetonitrile. Yield: 80%, m.p. 277 °C (dec.). *Anal.* Calc. for C<sub>36</sub>H<sub>24</sub>AuFeN<sub>8</sub>O<sub>2</sub>S<sub>4</sub> **1**: C, 43.87; H, 2.86; N, 11.37; S, 13.01. Found: C, 43.32; H, 3.15; N, 11.17; S, 11.47%. IR (KBr, cm<sup>−1</sup>)  $\nu$  = 3267 (N–H, w) 2219 (C≡N, s), 1640(C=N, s), 530(Fe–N, w), 440(Fe–O, w), 400(Fe–O, w), 350 (Au–S, w).

#### 2.1.2. [Fe(sal<sub>2</sub>-trien)] [Ni(dcbdt)<sub>2</sub>] (2)

A similar procedure as used for **1** was followed and 19.97 mg of black parallelepipedic crystals were obtained. Yield: 82%. *Anal.* Calc. for C<sub>35</sub>H<sub>24</sub>NiFeN<sub>8</sub>O<sub>2</sub>S<sub>4</sub> **2**: C, 51.27; H, 2.87; N, 13.29; S, 15.21. Found: C, 51.10; H, 2.51; N, 13.17; S, 15.27%.

#### 2.1.3. [Fe(phen)<sub>3</sub>] [Au(dcbdt)<sub>2</sub>]<sub>2</sub> · CH<sub>3</sub>CN (3)

A solution of [Fe(phen)<sub>3</sub>] (PF<sub>6</sub>)<sub>2</sub> (30.00 mg, 0.05 mmol) in 25 mL of acetonitrile was added dropwise to a solution of (*n*-Bu<sub>4</sub>N) [Au(dcbdt)<sub>2</sub>] (45.00 mg, 0.04 mmol), in the same amount of the same solvent. Slow evaporation gave

Table 1  
Crystallographic data and refinement details for compounds **2**, **3** and **4**

	[Fe(sal <sub>2</sub> -trien)] [Ni(dcbdt) <sub>2</sub> ] ( <b>2</b> )	[Fe(phen) <sub>3</sub> ] [Au(dcbdt) <sub>2</sub> ] <sub>2</sub> ( <b>3</b> )	[Fe(phen) <sub>3</sub> ] [Ni(dcbdt) <sub>2</sub> ] <sub>2</sub> ( <b>4</b> )
Empirical formula	C <sub>36</sub> H <sub>28</sub> N <sub>8</sub> O <sub>2</sub> S <sub>4</sub> FeNi	C <sub>70</sub> H <sub>35</sub> Au <sub>2</sub> FeN <sub>15</sub> S <sub>8</sub>	C <sub>70</sub> H <sub>35</sub> FeN <sub>15</sub> Ni <sub>2</sub> S <sub>8</sub>
Formula weight	847.46	1792.39	1515.88
Temperature (K)	294(2)	150(2)	110(2)
Wavelength (Å)	0.71073	0.71073	0.71073
Crystal system, specific gravity	triclinic, P $\bar{1}$	triclinic, P $\bar{1}$	triclinic, P $\bar{1}$
<i>a</i> (Å)	7.9258(3)	9.4912(7)	9.3961(9)
<i>b</i> (Å)	14.5604(6)	12.2375(9)	12.1885(14)
<i>c</i> (Å)	17.042(7)	27.525(2)	27.565(3)
$\alpha$ (°)	76.5370(10)	83.263(5)	83.575(7)
$\beta$ (°)	76.0450(10)	89.455(5)	89.588(7)
$\gamma$ (°)	75.4980(10)	87.806(5)	88.038(7)
Volume (Å <sup>3</sup> )	1816.5(8)	3172.5(4)	3135.2(6)
<i>Z</i> , <i>D</i> <sub>calc</sub> (g/cm <sup>−3</sup> )	2, 1.549	2, 1.876	2, 1.606
<i>M</i> (mm <sup>−1</sup> )	1.194	5.161	1.149
<i>F</i> (000)	868	1744	1540
Crystal size (mm)	0.30 × 0.16 × 0.06	0.20 × 0.02 × 0.01	0.14 × 0.08 × 0.04
$\theta$ Range (°)	2.94–26.37	2.27–26.46	2.63–25.68
Limiting indices <i>hkl</i>	−6/9, −17/18, −21/21	−11/11, −15/15, −34/34	−11/11, −14/14, −33/33
Reflections collected	29801	48921	51740
Independent reflections [ <i>R</i> <sub>int</sub> ]	7377 [0.0602]	12959 [0.0943]	11895 [0.0903]
<i>T</i> <sub>max</sub> , min	0.9318, 0.7159	0.9502, 0.4250	0.9555, 0.8557
Data/restraints/parameters	7377/0/479	12959/0/866	11895/0/866
<i>S</i> on <i>F</i> <sup>2</sup>	0.971	0.939	1.044
<i>R</i> ( <i>I</i> > 2σ( <i>I</i> ))	<i>R</i> <sub>1</sub> = 0.0451, <i>wR</i> = 0.0965	<i>R</i> <sub>1</sub> = 0.0406, <i>wR</i> = 0.0666	<i>R</i> <sub>1</sub> = 0.0526, <i>wR</i> = 0.1051
<i>R</i> (all data)	<i>R</i> <sub>1</sub> = 0.0839, <i>wR</i> = 0.1074	<i>R</i> <sub>1</sub> = 0.0856, <i>wR</i> = 0.0740	<i>R</i> <sub>1</sub> = 0.0962, <i>wR</i> = 0.1164
$\Delta$ <sub>max</sub> , min (e Å <sup>−3</sup> )	0.469, −0.337	1.065, −0.908	2.469, −1.938

Table 2  
Selected bond lengths (Å) and angles (°) for compounds **2**, **3** and **4**

[Fe(sal <sub>2</sub> -trien)] [Ni(dcbdt) <sub>2</sub> ]		[Fe(phen) <sub>3</sub> ] [Au(dcbdt) <sub>2</sub> ] <sub>2</sub>		[Fe(phen) <sub>3</sub> ] [Ni(dcbdt) <sub>2</sub> ] <sub>2</sub>	
Ni(1)–S(2)	2.1386(8)	Au(1)–S(1)	2.2982(16)	Ni(1)–S(1)	2.1411(12)
Ni(1)–S(3)	2.1447(8)	Au(1)–S(3)	2.3036(16)	Ni(1)–S(2)	2.1511(12)
Ni(1)–S(4)	2.1471(10)	Au(1)–S(2)	2.3067(16)	Ni(1)–S(3)	2.1474(12)
Ni(1)–S(1)	2.1530(10)	Au(1)–S(4)	2.3073(15)	Ni(1)–S(4)	2.1497(12)
S(1)–C(1)	1.729(3)	Au(2)–S(5)	2.3070(17)	Ni(2)–S(5)	2.1504(12)
S(2)–C(2)	1.719(3)	Au(2)–S(8)	2.3120(16)	Ni(2)–S(6)	2.1659(13)
S(3)–C(9)	1.728(3)	Au(2)–S(6)	2.3165(16)	Ni(2)–S(7)	2.1695(13)
S(4)–C(10)	1.732(3)	Au(2)–S(7)	2.3186(17)	Ni(2)–S(8)	2.1624(13)
		S(1)–C(1)	1.749(6)	S(1)–C(1)	1.724(4)
		S(2)–C(2)	1.751(6)	S(2)–C(2)	1.735(4)
		S(3)–C(9)	1.749(6)	S(3)–C(9)	1.725(4)
		S(4)–C(10)	1.754(6)	S(4)–C(10)	1.731(4)
		S(5)–C(17)	1.741(6)	S(5)–C(17)	1.740(4)
		S(6)–C(18)	1.746(6)	S(6)–C(18)	1.740(4)
		S(7)–C(22)	1.737(6)	S(7)–C(25)	1.748(4)
		S(8)–C(23)	1.743(6)	S(8)–C(26)	1.734(4)
Fe(1)–O(1)	1.880(2)	Fe(1)–N(9)	1.963(4)	Fe(1)–N(14)	1.988(3)
Fe(1)–O(2)	1.896(2)	Fe(1)–N(10)	1.970(5)	Fe(1)–N(13)	1.990(3)
Fe(1)–N(8)	2.031(3)	Fe(1)–N(11)	1.970(5)	Fe(1)–N(11)	1.990(3)
Fe(1)–N(5)	2.049(3)	Fe(1)–N(14)	1.972(5)	Fe(1)–N(9)	1.992(3)
Fe(1)–N(7)	2.107(3)	Fe(1)–N(12)	1.980(4)	Fe(1)–N(12)	1.999(3)
Fe(1)–N(6)	2.125(3)	Fe(1)–N(13)	1.984(5)	Fe(1)–N(10)	2.000(3)
S(2)–Ni(1)–S(3)	175.67(4)	S(1)–Au(1)–S(3)	88.01(6)	S(1)–Ni(1)–S(3)	86.93(5)
S(2)–Ni(1)–S(4)	86.72(3)	S(1)–Au(1)–S(2)	90.12(6)	S(1)–Ni(1)–S(4)	171.86(5)
S(3)–Ni(1)–S(4)	92.12(3)	S(3)–Au(1)–S(2)	174.83(6)	S(3)–Ni(1)–S(4)	92.41(5)
S(2)–Ni(1)–S(1)	92.22(3)	S(1)–Au(1)–S(4)	175.55(6)	S(1)–Ni(1)–S(2)	92.20(5)
S(3)–Ni(1)–S(1)	89.14(3)	S(3)–Au(1)–S(4)	90.01(6)	S(3)–Ni(1)–S(2)	174.02(5)
S(4)–Ni(1)–S(1)	176.94(4)	S(2)–Au(1)–S(4)	92.18(6)	S(4)–Ni(1)–S(2)	89.28(4)
		S(5)–Au(2)–S(8)	179.62(6)	S(5)–Ni(2)–S(8)	178.80(6)
		S(5)–Au(2)–S(6)	89.42(6)	S(5)–Ni(2)–S(6)	91.88(5)
		S(8)–Au(2)–S(6)	90.95(6)	S(8)–Ni(2)–S(6)	88.00(5)
		S(5)–Au(2)–S(7)	89.99(6)	S(5)–Ni(2)–S(7)	89.13(5)
		S(8)–Au(2)–S(7)	89.65(6)	S(8)–Ni(2)–S(7)	90.96(5)
		S(6)–Au(2)–S(7)	179.37(6)	S(6)–Ni(2)–S(7)	178.53(5)
O(1)–Fe(1)–O(2)	101.09(11)	N(9)–Fe(1)–N(10)	82.7(2)	N(14)–Fe(1)–N(13)	82.22(13)
O(1)–Fe(1)–N(8)	90.76(11)	N(9)–Fe(1)–N(11)	92.6(2)	N(14)–Fe(1)–N(11)	174.78(14)
O(2)–Fe(1)–N(8)	89.41(11)	N(10)–Fe(1)–N(11)	92.3(2)	N(13)–Fe(1)–N(11)	94.21(13)
O(1)–Fe(1)–N(5)	89.47(11)	N(9)–Fe(1)–N(14)	3.36(19)	N(14)–Fe(1)–N(9)	92.43(14)
O(2)–Fe(1)–N(5)	89.07(11)	N(10)–Fe(1)–N(14)	174.6(2)	N(13)–Fe(1)–N(9)	92.71(14)
N(8)–Fe(1)–N(5)	178.48(11)	N(11)–Fe(1)–N(14)	91.57(19)	N(11)–Fe(1)–N(9)	91.54(13)
O(1)–Fe(1)–N(7)	90.18(11)	N(9)–Fe(1)–N(12)	174.0(2)	N(14)–Fe(1)–N(12)	93.96(14)
O(2)–Fe(1)–N(7)	164.85(12)	N(10)–Fe(1)–N(12)	93.94(19)	N(13)–Fe(1)–N(12)	93.00(13)
N(8)–Fe(1)–N(7)	80.27(12)	N(11)–Fe(1)–N(12)	82.5(2)	N(11)–Fe(1)–N(12)	82.39(13)
N(5)–Fe(1)–N(7)	101.23(11)	N(14)–Fe(1)–N(12)	90.30(19)	N(9)–Fe(1)–N(12)	171.96(13)
O(1)–Fe(1)–N(6)	163.32(11)	N(9)–Fe(1)–N(13)	93.19(19)	N(14)–Fe(1)–N(10)	93.73(13)
O(2)–Fe(1)–N(6)	91.23(10)	N(10)–Fe(1)–N(13)	93.8(2)	N(13)–Fe(1)–N(10)	173.42(14)
N(8)–Fe(1)–N(6)	100.67(11)	N(11)–Fe(1)–N(13)	172.0(2)	N(11)–Fe(1)–N(10)	90.16(13)
N(5)–Fe(1)–N(6)	79.43(11)	N(14)–Fe(1)–N(13)	82.6(2)	N(9)–Fe(1)–N(10)	82.24(14)
N(7)–Fe(1)–N(6)	79.94(11)	N(12)–Fe(1)–N(13)	91.97(19)	N(12)–Fe(1)–N(10)	92.46(14)

59.42 mg of black parallelepipedic crystals which were washed with cold acetonitrile. Yield: 83%, m.p. >350 °C. *Anal.* Calc. for C<sub>70</sub>H<sub>36</sub>Au<sub>2</sub>FeN<sub>15</sub>S<sub>8</sub> **3**: C, 46.64; H, 1.84; N, 11.20; S, 14.65. Found: C, 46.16; H, 1.94; N, 11.24; S, 14.02%. IR (KBr, cm<sup>−1</sup>)  $\nu$  = 2221(C≡N, s), 430 (Fe–N, w), 350 (Au–S, w).

#### 2.1.4. [Fe(phen)<sub>3</sub>] [Ni(dcbdt)<sub>2</sub>]<sub>2</sub> · CH<sub>3</sub>CN (**4**)

A similar procedure as described for **3** was used and 36.13 mg of black parallelepipedic crystals were obtained.

Yield: 50%, m.p. >350 °C. *Anal.* Calc. for C<sub>70</sub>H<sub>36</sub>FeN<sub>15</sub>–Ni<sub>2</sub>S<sub>8</sub> **4**: C, 55.38; H, 2.19; N, 13.30; S, 17.39. Found C, 55.46; H, 2.66; N, 13.34; S, 17.22%. IR (KBr, cm<sup>−1</sup>)  $\nu$  = 2219 (C≡N, s), 420 (Ni–S, w), 400 (Fe–N, w).

#### 2.2. X-ray diffraction

X-ray diffraction experiments were performed with a Bruker AXS APEX CCD detector diffractometer using graphite monochromated Mo K $\alpha$  radiation ( $\lambda$  = 0.71073

Å), in the  $\phi$  and  $\omega$  scans mode. A semiempirical absorption correction was carried out using SADABS [9]. Data collection, cell refinement and data reduction were done with the SMART and SAINT programs [10]. The structures were solved by direct methods using SIR97 [11] and refined by fullmatrix least-squares methods using the program SHELXL97 [12] using the WINGX software package [13]. Non-hydrogen atoms were refined with anisotropic thermal parameters, whereas H-atoms were placed in idealized positions and allowed to refine riding on the parent C atom. Molecular graphics were prepared using ORTEP 3 [14]. A summary of the crystal data, structure solution and refinement is given in Table 1. Selected bond distances and angles are listed in Table 2.

### 2.3. Magnetic measurements

Magnetic measurements by a DC extraction method were performed on polycrystalline samples (20–30 mg) using a multipurpose characterization system, *MagLab 2000* (Oxford Instruments) with a 12 T magnet. The temperature dependence of the magnetic susceptibility in the temperature range 1.7–350 K was measured under a magnetic field of 5 T. The paramagnetic susceptibility was obtained from the experimental magnetization data after a diamagnetism correction was estimated from the tabulated Pascal constants as  $-390 \times 10^{-6}$ ,  $-352 \times 10^{-6}$ ,  $-851 \times 10^{-6}$  and  $-805 \times 10^{-6}$  emu/mol, for **1–4**, respectively.

## 3. Results and discussion

[Fe(sal<sub>2</sub>-trien)][Ni(dcbdt)<sub>2</sub>] (**2**) crystallizes in the triclinic space group  $P\bar{1}$ ,  $Z = 2$ , with cell parameters  $a = 7.9258(3)$  Å,  $b = 14.5604(6)$  Å,  $c = 17.042(7)$  Å,  $\alpha = 76.5370(10)^\circ$ ,  $\beta = 76.0450(10)^\circ$ ,  $\gamma = 75.4980(10)^\circ$ ,  $V = 1816.5(8)$  Å<sup>3</sup>. The unit cell contains one [Fe(sal<sub>2</sub>-trien)] cation and one [Ni(dcbdt)<sub>2</sub>] anion both at general positions (Fig. 1). The Ni anions are arranged in closely spaced pairs generated by an inversion center at each cell corner, so that the dimerised [Ni(dcbdt)<sub>2</sub>]<sub>2</sub><sup>2-</sup> anions present an Ni over S overlap mode with the Ni atom presenting a square base pyramidal coordination geometry, with an apical Ni–S bond distance of 2.783(1) Å and an Ni–Ni distance of 4.124(1) Å.

In spite of this pair overlap mode the [Ni(dcbdt)<sub>2</sub>] anions are almost planar, (the atomic deviations from average molecular plane are less than 0.084 Å). The equatorial Ni–S bond lengths (2.145(1) Å, 2.147(1) Å, 2.139(1) Å, 2.153(1) Å) are typical of Ni<sup>III</sup> but slightly shorter than those found in TBA [Ni(dcbdt)<sub>2</sub>] (2.196 Å) in which the Ni anions were also dimerised but with much shorter apical Ni–S bond distance (2.396 Å) and with a heavier non-planar distortion [5a].

The dimeric [Ni(dcbdt)<sub>2</sub>]<sub>2</sub><sup>2-</sup> units are arranged side by side in ladders along  $a$  (Fig. 2). However besides the N3...H12–C12 hydrogen bond, there are no significant short contacts between the neighbouring dimers. Each

[Ni(dcbdt)<sub>2</sub>]<sup>2-</sup> anion is connected to four cations through several hydrogen bonds and short contacts (see Table 3).

The cations present the Fe atom in an octahedral coordination geometry with average Fe–N and Fe–O distances of 2.078(3) and 1.888(2) Å, respectively, comparable to those previously found for [Fe(sal<sub>2</sub>-trien)] [Ni(dmit)<sub>2</sub>]<sub>2</sub> in the high spin state (2.155(3) Å and 1.909(3) Å, respectively) [2a]. These values are clearly distinct from those found for the low spin state (1.966 Å and 1.874 Å). The cation also presents a noticeable disorder of the ethylenic carbon atom C28 among two positions with almost identical (0.57 and 0.43) occupation factors.

The crystal structure of **2** can be described as consisting of layers of anionic chains parallel to the  $a$ ,  $b$  plane alternating along  $c$  with layers of cations.

The Au analog [Fe(sal<sub>2</sub>-trien)][Au(dcbdt)<sub>2</sub>] (**1**) was found to crystallize in the same space group with cell parameters  $a = 7.4389(1)$  Å,  $b = 13.2805(2)$  Å,  $c = 19.4777(4)$  Å,  $\alpha = 107.397(1)^\circ$ ,  $\beta = 97.381(1)^\circ$ ,  $\gamma = 101.251(1)^\circ$ ,  $V = 1764.7(1)$  Å<sup>3</sup>. However, the poor crystal quality prevented a structural refinement.

The [Fe(phen)<sub>3</sub>][M(dcbdt)<sub>2</sub>]<sub>2</sub> salts with M = Au (**3**) and Ni (**4**) crystallize on the triclinic  $P\bar{1}$  space group with similar cell parameters as indicated in Table 1. These two compounds are isostructural and the unit cells, just differing on the origin choice, contain one [Fe(phen)<sub>3</sub>] cation, two [M(dcbdt)<sub>2</sub>] anions, and one acetonitrile solvent molecule, all at general positions (Fig. 3).

The geometry of the molecular units and their bond lengths present normal values (see Table 2). The two anions (A – Ni1, Au1 and B – Ni2, Au2) are almost planar, with a slightly larger distortion from planarity being noticed in anion A for both Ni and Au compounds. The atomic deviations from average molecular plane are less than 0.170, 0.163 Å (anions A) and 0.042, 0.052 Å (anions B) for Ni and Au, respectively.

The equatorial Ni–S bond lengths for anion A (2.1411(12), 2.1511(11), 2.1474(11), 2.1497(11) Å) and anion B (2.1504(12), 2.1659(13), 2.1695(13), 2.1624(13) Å) are identical to those of compound **2**. Anions A form pairs of regular chains along  $a$ . The parallel and out-of-registry chains in the pair are connected through side-by-side short S...S and S...C contacts in a zig-zag pattern (Fig. 4). Anions B are connected on their extremities by pairs of hydrogen bonds involving the cyano groups, forming chains along  $a + b$ . These anion chains are organized in a compact plane parallel to  $a$ ,  $b$  plane. Neighbouring chains are either connected by M...M and M...S short contacts, making dimers of [M(dcbdt)<sub>2</sub>]<sub>2</sub> with the metal in a square pyramidal coordination with apical M–S distances of 3.547(2) Å and 3.379(1) Å for Au and Ni, respectively, or connected by S...C and M–N close contacts (see Fig. 5 and Table 3). It should be mentioned that these apical M–S distances are significantly shorter than the sum of the Van der Waals radii, and shorter than the Ni–S apical distance observed in [Ni(dcbdt)<sub>2</sub>]<sub>2</sub> dimers in **2**. The cations separate the two types of anionic layers and also the pairs of chains of cations B.



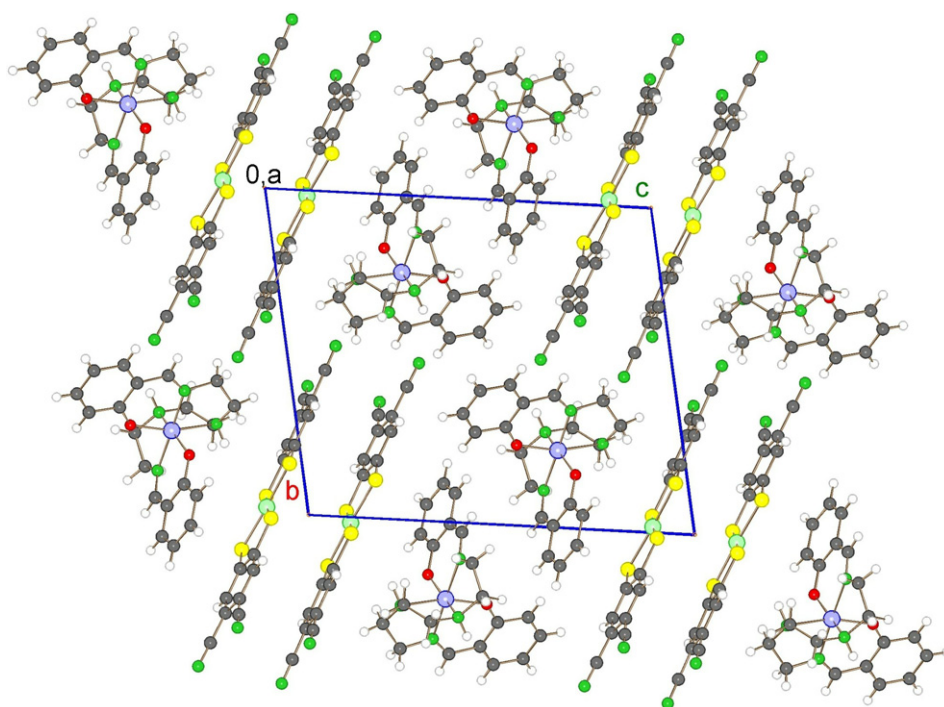


Fig. 1. Crystal structure of  $[\text{Fe}(\text{sal}_2\text{-trien})][\text{Ni}(\text{dcbdt})_2]$  (**2**) viewed along  $a$ .

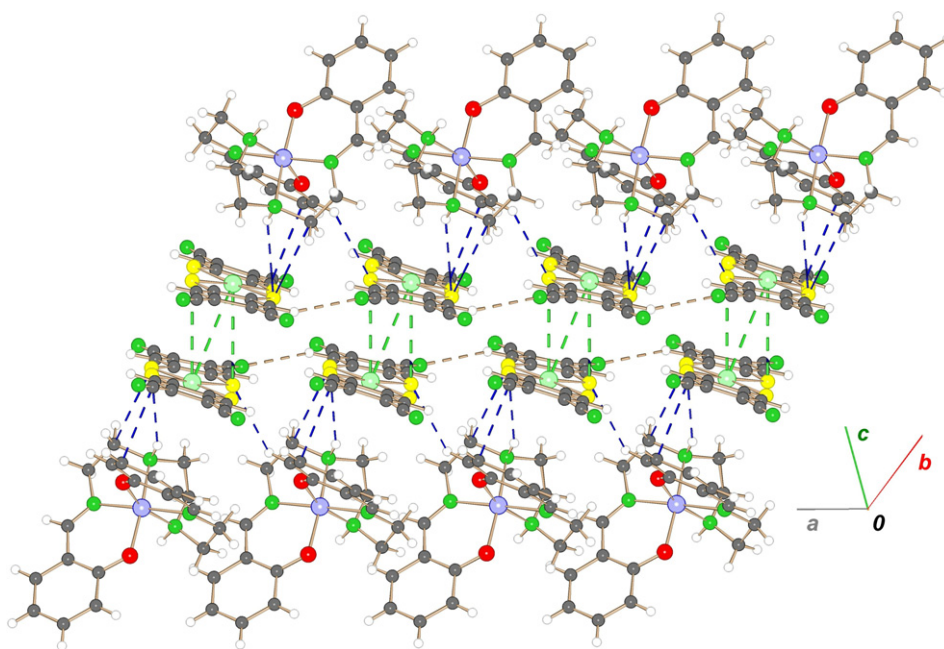


Fig. 2. Partial view of the crystal structure of **2** showing chains of  $[\text{Ni}(\text{dcbdt})_2]$  dimers sandwiched between  $[\text{Fe}(\text{sal}_2\text{-trien})]$  cations.

In compounds **3** and **4** the  $\text{Fe}(\text{phen})_3$  cation presents a quite regular octahedral geometry with  $\text{Fe-N}$  bond lengths ranging between 1.963(4) and 2.000(3) Å and inter-ligand  $\text{N-Fe-N}$  angles ranging between  $90.2(1)^\circ$  and  $94.2(1)^\circ$ . The angles between the normal to the ligand planes are  $78.5^\circ$ ,  $83.0^\circ$ ,  $86.0^\circ$  and  $78.9^\circ$ ,  $82.4^\circ$ ,  $86.3^\circ$  for compounds **3** and **4**, respectively. These values are typical of low spin Phenanthroline  $\text{Fe}(\text{II})$  complexes [15,16].

The magnetic properties of the  $[\text{Fe}(\text{sal}_2\text{-trien})][\text{M}(\text{dcbdt})_2]$  compounds with  $\text{M} = \text{Ni}$  and  $\text{Au}$  are expected to result from contributions of the cation, which a priori can be either in high  $S = 5/2$  (HS), low  $S = 1/2$  (LS) or intermediate  $S = 3/2$  spin states, in addition to a contribution from the  $S = 1/2$  Ni anion, while the Au anion is diamagnetic. The  $\chi T$  product for both Au and Ni salts are shown in Fig. 6. The fact that the effective magnetic

Table 3  
Short contacts in the crystal structure of compounds **2**, **3** and **4**

Compound ( <b>2</b> )	<i>d</i> (Å)	Compound ( <b>3</b> )	<i>d</i> (Å)	Compound ( <b>4</b> )	<i>d</i> (Å)
<i>Anion–anion</i>		<i>Anion A–anion A</i>		<i>Anion A–anion A</i>	
Ni1...Ni1	4.124(1) <sup>i</sup>	S1...S1	3.466(2)	S1...S1	3.634(2) <sup>i</sup>
Ni1...S3	3.783(1) <sup>i</sup>	S1...C3	3.474(7) <sup>i</sup>	S1...C15	3.385(6) <sup>ii</sup>
N3...H12	2.672 <sup>ii</sup>	S3...S3	3.485(2) <sup>ii</sup>	S3...S3	3.660(2) <sup>ii</sup>
S2...S2	3.734(1) <sup>iii</sup>	S3...C7	3.467(7) <sup>i</sup>	S3...C11	3.477(5) <sup>ii</sup>
		N3...H3	2.610 <sup>iii</sup>	N1...H11	2.604 <sup>i</sup>
<i>Anion–cation</i>		<i>Anion B–anion B</i>		<i>Anion B–anion B</i>	
N1...H6	2.297 <sup>iv</sup>	Au2...Au2	4.155(1) <sup>iii</sup>	Ni2...Ni2	4.085(1) <sup>iii</sup>
N2...H30	2.660 <sup>iv</sup>	Au2...S6	3.547(2) <sup>iii</sup>	Ni2...S7	3.379(1) <sup>iii</sup>
N4...H26A	2.569 <sup>v</sup>	Au2...C18	3.876(6) <sup>iii</sup>	Ni2...C25	3.666(4) <sup>iii</sup>
N4...H29A	2.622 <sup>vi</sup>	Au2...C24	3.802(6) <sup>iv</sup>	S5...C26	3.498(4) <sup>iii</sup>
		Au2...N6	3.745(6) <sup>iv</sup>	S7...C32	3.481(4) <sup>iv</sup>
<i>Cation–cation</i>		<i>S6...C23</i>		<i>S6...C23</i>	
C18...H24A	2.744 <sup>vii</sup>	N6...C31	3.455(6) <sup>iv</sup>	N6...C31	3.189(6) <sup>v</sup>
C20...H25A	2.888 <sup>viii</sup>	N6...H27	3.225(9) <sup>v</sup>	N6...H27	2.702 <sup>v</sup>
C21...H25A	2.884 <sup>viii</sup>	N7...C24	2.707 <sup>v</sup>	N7...C24	2.702 <sup>v</sup>
		N7...H20	3.194(9) <sup>vi</sup>	N7...C24	3.225(9) <sup>vi</sup>
		N7...H20	2.653 <sup>vi</sup>		
		<i>Anion–cation</i>		<i>Anion–cation</i>	
		H37...N1	2.527 <sup>vii</sup>	H67...N3	2.497 <sup>vii</sup>
		H41...N2	2.654 <sup>viii</sup>	H52...S2	2.939 <sup>viii</sup>
		C59...S4	3.488(6) <sup>ix</sup>	H4...H35	2.388 <sup>iv</sup>
		H59...S4	2.839 <sup>ix</sup>	H12...C33	2.609 <sup>ix</sup>
		H62...S5	2.928 <sup>x</sup>	H12...C34	2.598 <sup>ix</sup>
		H64...S7	2.996 <sup>x</sup>	H57...N5	2.626 <sup>iii</sup>
		H52...N5	2.686 <sup>xi</sup>	H46...N7	2.453 <sup>iii</sup>
		H66...N5	2.421 <sup>xii</sup>	H45...N8	2.451 <sup>iii</sup>
		H65...N6	2.468 <sup>xii</sup>	H40...N8	2.639 <sup>x</sup>
		H33...N8	2.688 <sup>xiii</sup>	H55...S8	2.899 <sup>vi</sup>
		<i>Cation–cation</i>		<i>Cation–cation</i>	
		C38...H40	2.893 <sup>xiv</sup>	C32...H40	2.796 <sup>xi</sup>
		C52...H46	2.880 <sup>xv</sup>	C40...H34	2.806 <sup>x</sup>
		H52...H46	2.380 <sup>xv</sup>	C68...H64	2.879 <sup>xii</sup>
				H34...H40	2.322 <sup>xi</sup>

Symmetry codes for compound **2**: <sup>i</sup>−*x* + 2, −*y*, −*z*; <sup>ii</sup>*x* + 1, +*y*, +*z*; <sup>iii</sup>−*x* + 1, −*y*, −*z*; <sup>iv</sup>*x*, +*y* − 1, +*z*; <sup>v</sup>−*x* + 2, −*y* + 1, −*z*; <sup>vi</sup>−*x* + 1, −*y* + 1, −*z*; <sup>vii</sup>*x* − 1, +*y*, +*z*; <sup>viii</sup>−*x* + 1, −*y*, −*z* + 1.

Symmetry codes for compound **3**: <sup>i</sup>−*x*, −*y* + 1, −*z* + 1; <sup>ii</sup>−*x* + 1, −*y* + 1, −*z* + 1; <sup>iii</sup>−*x*, −*y* + 1, −*z* + 2; <sup>iv</sup>−*x* + 1, −*y* + 1, −*z* + 2; <sup>v</sup>*x* + 1, +*y* − 1, +*z*; <sup>vi</sup>*x* − 1, +*y* + 1, +*z*; <sup>vii</sup>−*x* − 1, −*y*, −*z* + 1; <sup>viii</sup>*x* + 1, +*y*, +*z*; <sup>ix</sup>, +*y* − 1, +*z*; <sup>x</sup>*x*, +*y* − 1, +*z* − 1; <sup>xi</sup>*x*, +*y*, +*z* − 1; <sup>xii</sup>*x* − 1, +*y*, +*z* − 1; <sup>xiii</sup>−*x* − 1, −*y* + 1, −*z* + 1; <sup>xiv</sup>−*x*, −*y*, −*z* + 1; <sup>xv</sup>*x* + 1, +*y*, +*z*.

Symmetry codes for compound **4**: <sup>i</sup>−*x* + 1, −*y* + 1, −*z*; <sup>ii</sup>−*x* + 2, −*y* + 1, −*z*; <sup>iii</sup>−*x*, −*y* + 1, −*z* + 1; <sup>iv</sup>−*x* + 1, −*y* + 1, −*z* + 1; <sup>v</sup>*x* − 1, +*y* + 1, +*z*; <sup>vi</sup>*x* + 1, +*y* − 1, +*z*; <sup>vii</sup>*x* − 1, +*y* − 1, +*z* + 1; <sup>viii</sup>−*x* + 2, −*y*, −*z* + 1; <sup>ix</sup>−*x* + 2, −*y* + 1, −*z* + 1; <sup>x</sup>*x* + 1, *y*, *z*; <sup>xi</sup>*x* − 1, +*y*, +*z*; <sup>xii</sup>−*x* + 2, −*y*, −*z* + 2.

moment of the Ni salt is comparable to the Au one with diamagnetic anions, suggests that the paramagnetic contribution of the [Ni(dcbdt)<sub>2</sub>] anions is negligible due to their strong dimerisation, previously described, which leads to a singlet *S* = 0 ground state in the anionic sub-lattice. The crystallographic data are consistent with Fe<sup>III</sup> in a *S* = 5/2 state.

For [Fe(sal<sub>2</sub>-trien)] [Au(dcbdt)<sub>2</sub>] (**1**)  $\chi T \approx 4.0$  emu K/mol at 300 K, close to the value expected for an *S* = 5/2 system with *g* = 2 (4.37 emu K/mol). The  $\chi T$  product shows a slight increase as the temperature decreases down

to 30 K where it reaches a maximum  $\approx 4.5$  emu K/mol. The decrease of  $\chi T$  at lower temperatures (*T* < 20 K) is a consequence of the high field employed in the measurements (5 T). Indeed AC susceptibility measurements under zero field (not shown) display a similar maximum of  $\chi T$  but around 6 K suggesting that above this temperature the AF interactions become progressively more important. Upon heating–cooling cycles no jump or hysteresis loop characteristic of spin transition is observed in the magnetization, which suggests that this sample remains mainly in the high-spin state. However there is a small, but significant, thermal hysteresis that is observed in the range, possibly associated with a minor structural change. The magnetization curve *M*(*B*), obtained at 1.7 K (Fig. 7) approaches a saturation value of 4.7  $\mu_B$ /mol at 12 T, close to the value of 4.8  $\mu_B$ /mol expected for a system of *S* = 5/2 spins with *g* = 2. However, it is noticeable that the magnetization follows under the calculated Brillouin function denoting the presence of AF interactions at this low temperature in agreement with a decrease of the AC  $\chi T$  below 6 K.

For [Fe(sal<sub>2</sub>-trien)] [Ni(dcbdt)<sub>2</sub>] (**2**) the  $\chi T$  product is close to 3.8 emu K/mol at room temperature and it is almost temperature independent down to 30 K (Fig. 6), with a very slight tendency to decrease upon cooling. At room temperature there is a small but reproducible step variation of  $\approx 5\%$  in the  $\chi T$  product which can be associated with a structural change in the lattice, possibly the onset of motion of the ethylenic carbon atom C28 in the cation ligand, changing from a static to a dynamic disorder situation at higher temperatures. Cooling–warming cycles, give approximately the same values of magnetization, which apart from the small step previously mentioned are almost constant in the temperature range of 20–350 K, with no sign of spin crossover or equilibrium between HS and LS ground states.

Although the  $\chi T$  value is lower than the expected value for the *S* = 5/2 cations with *g* = 2, and slightly lower from the Au analog, the fact that these two compounds **1** and **2** present comparable  $\chi T$  values indicates not only that the Ni sublattice contribution is negligible due to the formation of strong anionic dimers, but also that the interaction between the cations and anions leads to stronger AF interaction. The enhanced AF interactions are also denoted by the magnetization curve *M*(*B*), at 1.7 K (Fig. 7) which approaches at 12 T a saturation value of 4.5  $\mu_B$ /mol, slightly smaller than the Au analog and also following below the Brillouin function for *S* = 5/2 and *g* = 2, but clearly above the *S* = 3/2 curve.

The magnetic behaviours of compounds [Fe(phen)<sub>3</sub>] [M(dcbdt)<sub>2</sub>]<sub>2</sub> with M = Au (**3**), Ni (**4**) are shown in Figs. 8 and 9. The fact that both Ni and Au salts have comparable magnetic susceptibility values, as for **1** and **2**, indicates that the *S* = 1/2 spins of the Ni anions are strongly antiferromagnetically coupled. This is consistent with the structural data. As previously described in the structures of **3** and **4** there are two type of anions, one forming pairs of

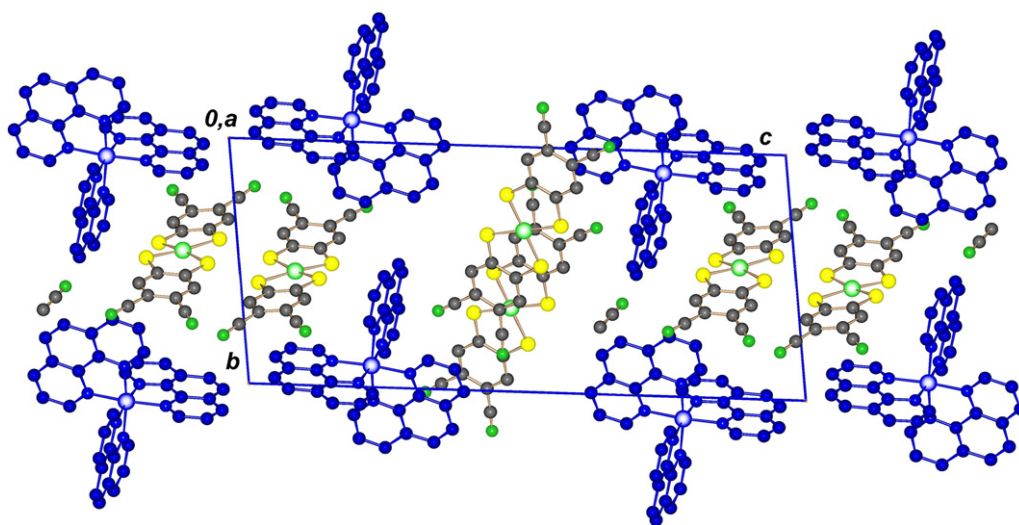


Fig. 3. Crystal structure of  $[\text{Fe}(\text{phen})_3][\text{Ni}(\text{dcbdt})_2]$  (**4**) viewed along  $a$ .

closely spaced regular chains and the other forming a bidimensional network of parallel chains. Both of these networks, if antiferromagnetically coupled, are expected to lead to a diamagnetic singlet ground state, as observed.

The  $\chi T$  product for the Ni and Au salts above 30 K are almost temperature independent with values  $\approx 1$  emu

K/mol and 0.9 emu K/mol respectively (Fig. 8). These values were found to be slightly dependent on the sample preparation. Since the Au anions are diamagnetic this significant paramagnetism clearly comes from the  $\text{Fe}^{\text{II}}$  cations that cannot be entirely in a  $S = 0$  state. These  $\chi T$  values are close to the value of 1.0 emu K/mol, expected for a  $S = 1$  state with  $g = 2$ . However since the  $S = 1$  state is unlikely to occur in a pseudo octahedral geometry most probably we have a low spin  $S = 0$  state with variable amounts up to ca. 25%, depending on the sample preparation, in the high spin  $S = 2$  state.

In fact as previously mentioned the observed metal–ligand distances, in particular, the N–Fe bond lengths are closer to the ones obtained for  $\text{Fe}^{\text{II}}$  phenanthroline complexes with low spin state [15,16]. An intermediate  $S = 1$  spin state is not so common for  $\text{Fe}^{\text{II}}$  phenanthroline complexes and it is not expected to occur in pseudo octahedral coordination geometry. In fact an incomplete and dependent on the preparation technique conversion to the low spin state has been previously described to occur in Fe phenanthroline complexes [15]. The decrease of  $\chi T$  observed for both compounds below 20 K is due to the large field (5 T) used for the measurements. AC magnetic susceptibility measurements under zero field (not shown) indicate that this value remains constant down to lower temperatures, but below 6 and 14 K for **3** and **4**, respectively, there is a reduction of the  $\chi T$  value that approaches 0.5 emu K/mol at 1.7 K.

On performing a warming–cooling cycle the presence of a small hysteresis in two different ranges of temperature, 150–250 K and 290–350 K is noticed. These hystereses are however too small to be ascribed to a spin transition and the results rather suggest that this sample remains mainly in an incompletely converted low spin state. Again we observe in these two compounds as in **1** and **2** that the paramagnetic Ni sub-lattices in spite of its antiferromagnetic coupled nature, contribute to enhance the AF coupling between the Fe centers.

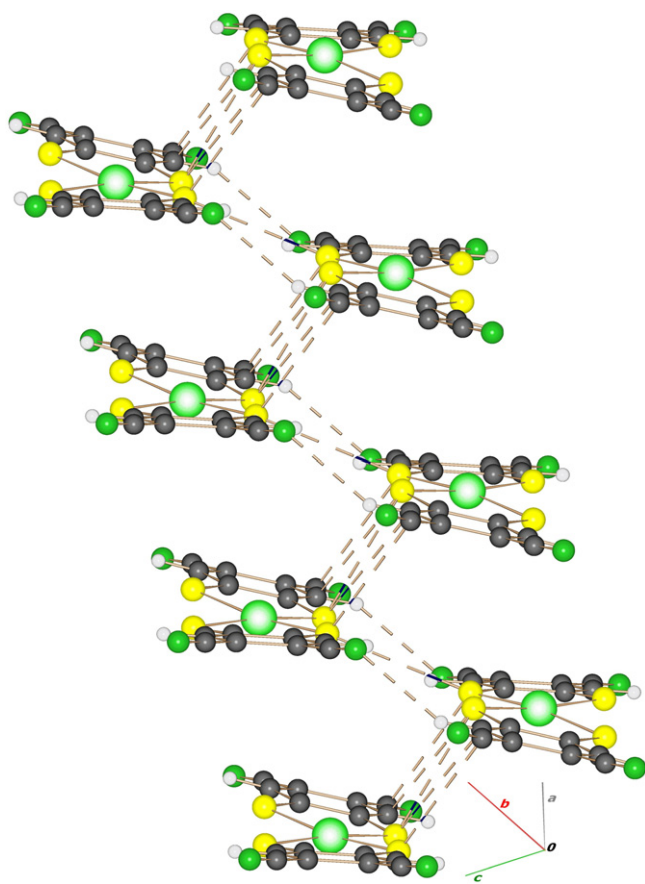


Fig. 4. Anions A in **4** connected through a zig-zag pattern of side-by-side short  $\text{S} \cdots \text{S}$  and  $\text{S} \cdots \text{C}$  contacts.



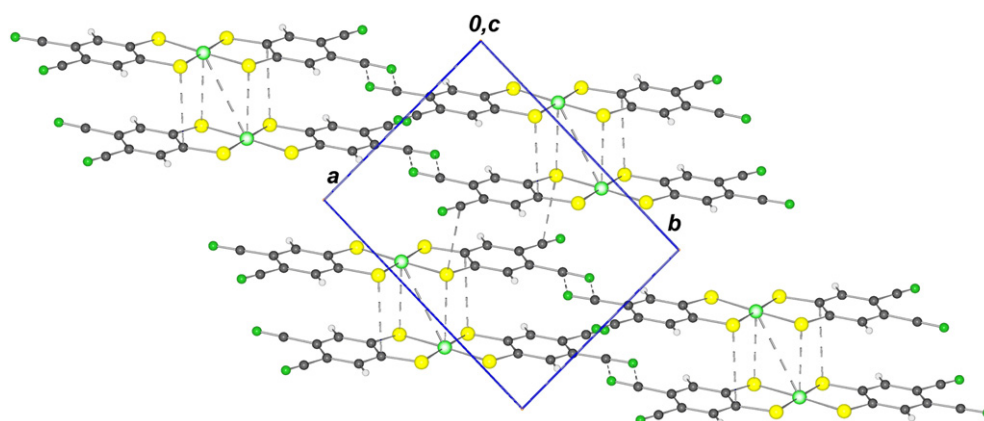


Fig. 5. View along  $c$  of a plane of anions B in **4**.

The magnetization curves of these compounds at 1.7 and 5 K are shown in Fig. 9. At the lower temperature, 1.7 K, the magnetization of Au compound **3** reaches a sat-

uration value of  $1.18 \mu_B$  above 5 T, consistent with an incompletely converted ( $\sim 25\%$ ) low spin state.

Ni compound **4** magnetisation increases with field in a slower fashion and although with values at 12 T

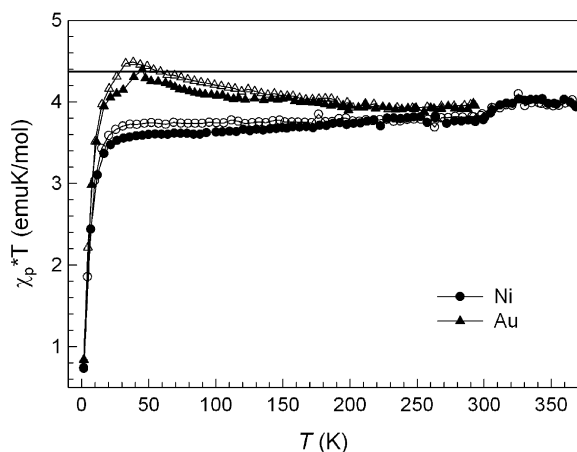


Fig. 6.  $\chi T$  vs.  $T$ , under 5 T of the  $[\text{Fe}(\text{salt}_2 \text{trien})][\text{M}(\text{dcbdt})_2]$  compounds **1** and **2**. Open symbols cooling, solid symbols warming. The solid line represents the expected value for Fe in the  $S = 5/2$  configuration with  $g = 2$ .

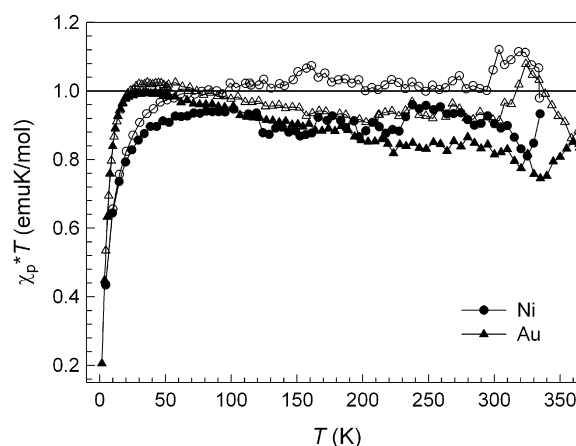


Fig. 8.  $\chi T$  vs.  $T$ , under 5 T of the  $[\text{Fe}(\text{phen})_3][\text{M}(\text{dcbdt})_2]$  compounds **3** and **4**. Open symbols cooling, solid symbols warming. The solid line represents the expected value of  $\chi T$  for  $\text{Fe}^{\text{II}}$  in the  $S = 1$  configuration with  $g = 2$ .

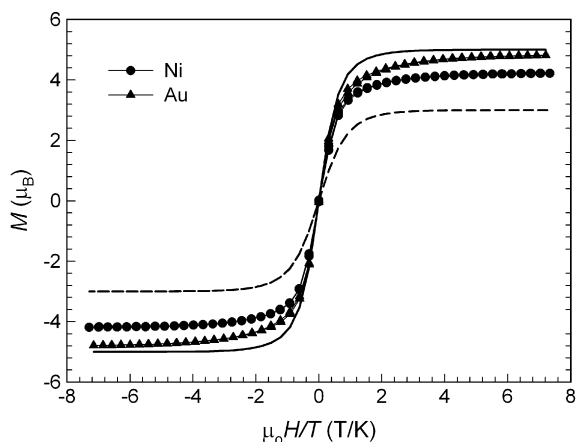


Fig. 7. Magnetic field dependence of the magnetization at 1.7 K of the  $[\text{Fe}(\text{salt}_2\text{-trien})][\text{M}(\text{dcbdt})_2]$  complexes **1** and **2**. The lines represent the Brillouin function for  $S = 3/2$  (dashed) and  $S = 5/2$  (solid) configurations with  $g = 2$ .

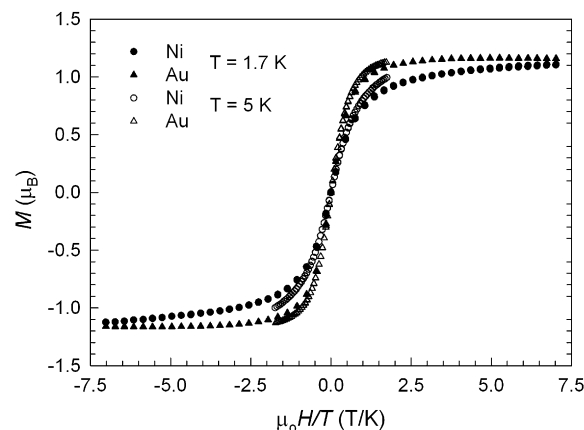


Fig. 9. Magnetic field dependence of the magnetization of the  $[\text{Fe}(\text{phen})_3][\text{M}(\text{dcbdt})_2]$  compounds **3** and **4** for fields up to 12 T measured at 1.7 K (closed symbols) and 5 K (open symbols).

comparable to Au compound **3** the magnetization at this field seems not yet entirely saturated. These results confirm that the paramagnetic Ni sub-lattices contribute to enhance the AF coupling between the Fe centers.

#### 4. Conclusion

In conclusion we have prepared and characterized four new salts of the monoanions  $[M(\text{dcbdt})_2]^-$  with  $M = \text{Au}$  and  $\text{Ni}$ . The magnetic properties of these compounds are dominated by the  $\text{Fe}^{\text{III}}$  and  $\text{Fe}^{\text{II}}$  cations contribution, in high spin ( $S = 5/2$ ) and low spin configurations respectively. None of these salts shows clear spin crossover behaviour. The absence of a clear spin transition is most probably the result of a very rigid crystal lattice.

The  $M = \text{Ni}$  compounds present a negligible contribution of the anionic sublattice to the bulk magnetization that is close to that of the analogous compounds with diamagnetic ( $M = \text{Au}$ ) anionic sublattice. This is due to strong antiferromagnetic interactions between the  $S = 1/2$  Ni anions. However, the anions enhance the AF interactions in the cation sublattice. The preparation of salts of these cations with partially oxidized anions, possibly electronic conductors, is presently being explored by us and will be reported in due time.

#### Acknowledgement

This work was benefited from the support of COST action D35 and EC MAGMANet network of excellence.

#### Appendix A. Supplementary material

CCDC 626997, 626995 and 626996 contain the supplementary crystallographic data for **2**, **3** and **4**. These data can be obtained free of charge via <http://www.ccdc.cam.ac.uk/conts/retrieving.html>, or from the Cambridge Crystallographic Data Centre, 12 Union Road, Cambridge CB2 1EZ, UK; fax: (+44) 1223-336-033; or e-mail: deposit@ccdc.cam.ac.uk. Supplementary data associated with this

article can be found, in the online version, at [doi:10.1016/j.ica.2007.03.015](https://doi.org/10.1016/j.ica.2007.03.015).

#### References

- [1] For recent reviews see for instance: (a) A.B. Gaspar, V. Ksenofontov, M. Seredyuk, P. Gutlich, *Coord. Chem. Rev.* 249 (2005) 266; (b) P.J. van Koningsbruggen, Y. Maeda, H. Oshio, *Top. Curr. Chem.* 233 (2004) 259.
- [2] (a) S. Dorbes, L. Valade, J.A. Real, C. Faulmann, *Chem. Comm.* 1 (2005) 69; (b) C. Faulmann, S. Dorbes, J.A. Real, L. Valade, *J. Low Temp. Phys.* 142 (2006) 26.
- [3] (a) K. Takahashi, H.B. Cui, Y. Okano, *Inorg. Chem.* 45 (2006) 5739; (b) K. Takahashi, H.B. Cui, H. Kobayashi, Y. Einaga, O. Sato, *Chem. Lett.* 34 (2005) 1240.
- [4] (a) P. Cassoux, J. Miller, in: L.V. Interrante, M.J. Hampden-Smith (Eds.), *Chemistry of Advanced Materials: An Overview*, New York, USA, 1998, p.19; (b) C. Faulmann, P. Cassoux, *Prog. Inorg. Chem.* 52 (2004); (c) P. Cassoux, L. Valade, in: D.W. Bruce, D. O'Hare (Eds.), *Inorganic Materials*, second ed., John Wiley and Sons, Chichester, 1996, p. 1264.
- [5] (a) D. Simão, H. Alves, D. Belo, S. Rabaça, E.B. Lopes, V. Gama, M.T. Duarte, R.T. Henriques, H. Novais, M. Almeida, *Eur. J. Inorg. Chem.* 12 (2001) 3119; (b) H. Alves, D. Simão, I.C. Santos, V. Gama, R.T. Henriques, H. Novais, M. Almeida, *Eur. J. Inorg. Chem.* 6 (2004) 1318.
- [6] (a) H. Alves, D. Simão, E.B. Lopes, V. Gama, M.T. Duarte, H. Novais, R.T. Henriques, M. Almeida, *Synth. Metals* 120 (2001) 1011; (b) H. Alves, I.C. Santos, E.B. Lopes, D. Belo, V. Gama, D. Simão, H. Novais, M.T. Duarte, R.T. Henriques, M. Almeida, *Synth. Metals* 133 (2003) 397.
- [7] M.F. Tweedle, L.J. Wilson, *J. Am. Chem. Soc.* 98 (1976) 4824.
- [8] S. Decurtins, H.W. Schmalle, R. Pellaux, P. Schneuwly, A. Hauser, *Inorg. Chem.* 35 (1996) 1451.
- [9] G.M. Sheldrick, *SADABS*, Bruker AXS Inc., Madison, Wisconsin, USA, 2004.
- [10] Bruker, *SMART and SAINT*, Bruker AXS Inc., Madison, Wisconsin, USA, 2004.
- [11] A. Altomare, M.C. Burla, M. Camalli, G. Cascarano, G. Giacovazzo, A. Guagliardi, A.G.G. Moliterni, G. Polidori, R. Spagna, *J. Appl. Cryst.* 32 (1999) 115.
- [12] G.M. Sheldrick, *SHELXL97*, Program for Crystal Structure Refinement, University of Göttingen, Germany, 1997.
- [13] L.J. Ferrugia, *J. Appl. Cryst.* 32 (1999) 837.
- [14] L.J. Ferrugia, *J. Appl. Cryst.* 30 (1997) 565.
- [15] B. Gallois, J.-A. Real, C. Hauw, J. Zarembowitch, *Inorg. Chem.* 29 (1990) 1152.
- [16] C. Horn, M. Scudder, I. Dance, *Crys. Eng. Comm.* 1 (2001) 1.